Nogo-A Regulates Neural Precursor Migration in the Embryonic Mouse Cortex

Carole Mathis, Aileen Schröter, Michaela Thallmair and Martin E. Schwab

Brain Research Institute, University of Zurich and Department of Biology, ETH Zurich, 8057 Zurich, Switzerland

Carole Mathis and Aileen Schröter have contributed equally to this work.

Address correspondence to Martin E. Schwab, PhD, Brain Research Institute, University of Zurich and Department of Biology, ETH Zurich, Winterthurerstrasse 190, CH-8057 Zurich, Switzerland. Email: schwab@hifo.uzh.ch.

Although Nogo-A has been intensively studied for its inhibitory effect on axonal regeneration in the adult central nervous system, little is known about its function during brain development. In the embryonic mouse cortex, Nogo-A is expressed by radial precursor/glial cells and by tangentially migrating as well as postmigratory neurons. We studied radially migrating neuroblasts in wild-type and Nogo-A knockout (KO) mouse embryos. In vitro analysis showed that Nogo-A and its receptor components NgR, Lingo-1, TROY, and p75 are expressed in cells emigrating from embryonic forebrain–derived neurospheres. Live imaging revealed an increased cell motility when Nogo-A was knocked out or blocked with antibodies. Antibodies blocking NgR or Lingo-1 showed the same motility-enhancing effect supporting a direct role of surface Nogo-A on migration. Bromodeoxyuridine (BrdU) labeling of embryonic day (E)15.5 embryos demonstrated that Nogo-A influences the radial migration of neuronal precursors. At E17.5, the normal transient accumulation of radially migrating precursors within the subventricular zone was not detectable in the Nogo-A KO mouse cortex. At E19, migration to the upper cortical layers was disturbed. These findings suggest that Nogo-A and its receptor complex play a role in the interplay of adhesive and repulsive cell interactions in radial migration during cortical development.

Keywords: corticogenesis, migration, neural precursor, Nogo-A

Introduction

Nogo-A was originally identified as a myelin protein that inhibits neurite outgrowth in the adult central nervous system (CNS) (Caroni and Schwab 1988; Spillmann et al. 1998; Chen et al. 2000; GrandPre et al. 2000; Prinjha et al. 2000). Its identification confirmed the concept that molecules expressed by oligodendrocytes inhibit axon regeneration in the adult brain and spinal cord (Schwab and Caroni 1988). This discovery was followed by intensive studies with the goal of developing new therapeutic strategies to enhance axon regeneration and functional recovery after CNS injury (Schwab 2004; Yiu and He 2006; Gonzenbach and Schwab 2008).

In addition to its oligodendrocyte expression, Nogo-A is also detected in neurons of both the peripheral nervous system and the CNS, in particular, during development (Josephson et al. 2001; Huber et al. 2002; Wang et al. 2002; Hunt et al. 2003; Mingorance et al. 2004; Dodd et al. 2005). Its neuronal functions remain largely elusive, however. During embryogenesis, a high expression of Nogo-A was reported in various species (Huber et al. 2002; O'Neill et al. 2004; Al Halabiah et al. 2005; Caltharp et al. 2007). Nogo-A is present in tangentially migrating cortical interneurons of mouse cortices (Tozaki et al. 2002; Richard et al. 2005; Mingorance-Le Meur et al. 2007). In chicken embryos, Nogo-A expression is observed in neural precursors during neural plate formation (Caltharp et al. 2007). Its localization in large projection neurons of the optic tectum and tectal-associated nuclei suggests a function of neuronal Nogo-A in neurite formation and synaptogenesis (Caltharp et al. 2007). So far, however, all these hypothetical roles of neuronal Nogo-A during development are based on correlations between its spatial and temporal expression pattern and corresponding developmental events. None of the proposed functions have been proven experimentally. The hypothesis that the growth inhibitory and growth cone repulsive membrane protein Nogo-A is involved in various developmental processes is plausible since such functions were found for many repulsive axonal guidance (Klein 2004; Martinez and Soriano 2005), extracellular matrix, and cell adhesion molecules (Hirano et al. 2003; Kadowaki et al. 2007). A recent study analyzing corticogenesis in Nogo-A, -B, and -C knockout (KO) mutants revealed a disturbed migration of early tangentially migrating cortical interneurons (Mingorance-Le Meur et al. 2007). In vitro, the authors also found an increase in axon branching and early polarization of cortical neurons obtained from Nogo-deficient mouse cortices. These results support the idea that Nogo proteins play important roles during corticogenesis.

Here, we studied the developing mouse cortex and found Nogo-A expressed in radial glia, radially and tangentially migrating as well as postmigratory neurons. In embryonic forebrain–derived neurospheres, Nogo-A and some known Nogo receptor components were found on the precursor cell surface. Live imaging analysis of the movement of neurosphere-derived cells demonstrated that Nogo-A acts as a negative regulator of cell motility. In addition, we show that the adhesion and spreading of neural precursor cells were influenced by a Nogo-A substrate. Bromodeoxyuridine (BrdU)-labeling experiments demonstrated that in vivo Nogo-A plays a role in different phases of the radial migration process, probably controlling adhesive and repulsive interactions between migratory cells and their vicinity. Our data suggest a new regulatory mechanism mediated by the Nogo-A/Nogo receptor pathway influencing neuronal precursor cell motility during cortical development.

Materials and Methods

Animals

All animal procedures were in strict accordance with the guidelines of the Veterinary Department of the canton of Zurich. Experiments were performed with brains from embryonic and newborn wild-type (WT) and Nogo-A KO C57BL/6 mice (Simonen et al. 2003). The morning of plug detection in females was considered as embryonic day (E)0.5. Pregnant mice were sacrificed by cervical dislocation, and embryonic brains were harvested for further processing. Genotypes were controlled by polymerase chain reaction (PCR) analysis of genomic DNA (Simonen et al. 2003). Embryonic brains of WT and Nogo-A KO mice were dissected at E15.5, E17.5, or E19; fixed in 4%

paraformaldehyde (PFA); and cryoprotected in 30% sucrose in phosphate buffer before embedding in OCT (Tissue-Tek, Sakura Finetek Europe B.V., Zoeterwoude, The Netherlands) at –40 °C. Brain coronal cryosections of 20 μm were cut and immunostained.

Immunohistochemistry and Cytochemistry

Primary antibodies: mouse, anti-APC (Anti-Adenomatus Polyposis Coli; 1:100; Calbiochem, Merck Chemicals Ltd., Nottingham, UK), anti-nestin (1:200; BD Pharmingen, BD Biosciences, CA), anti-tubulinβIII (TubβIII, 1:1000; Promega, Dübendorf, Switzerland), anti-Satb2 (1:50; Abcam, Cambridge, UK); rabbit, anti-Calbindin (1:2000; Swant, Bellinzona, Switzerland), anti-GFAP (glial fibrillary acidic protein; 1:2000; Dako, Glostrup, Denmark), anti-Lingo-1 (1:100; Abcam), anti-Nogo-A Rb173A (1:1000; Oertle et al. 2003; Dodd et al. 2005), anti-NgR (1:100; Alpha Diagnostic International, San Antonio, TX), anti-Pax6 (1:300; Covance), anti-p75 (1:100; Promega), anti-Tbr1 (1:1000; Millipore, Billerica, MA), anti-TROY (1:100; Santa Cruz Biotechnology Inc., Santa Cruz, CA); rat, anti-BrdU (1:500; Biozol, Eching, Germany); and goat, anti-doublecortin (Dcx, 1:500; Santa Cruz). Secondary antibodies: species-specific Cy3 or Cy5 or biotin conjugated followed by incubation with streptavidin-dichlorotriazinyl amino fluorescein (all 1:500; Jackson ImmunoResearch, Suffolk, UK). Cell nuclei were counterstained with DAPI (4′-6-diamidino-2-phenylindole) nuclear stain (1:1000; Sigma-Aldrich, Buchs, Switzerland). Slides were coverslipped with Mowiol (Sigma-Aldrich).

Fluorescent images of embryonic cortices or immunostained cells were acquired by conventional fluorescence microscopy (Axioskop; Zeiss, Carl Zeiss AG, Feldbach, Switzerland; Leica AF6000) or on a confocal microscope (Leica DMRE; Leica Microsystems, Wetzlar, Germany) using a 20× objective with an electronic zoom of 1.4-fold or a 40× oil immersion objective. Confocal z-stacks with a 63× oil immersion objective were acquired for analysis of the cell surface staining. Digitized images were further processed using Adobe Photoshop software.

Neurosphere Cultures, Reverse Transcriptase Polymerase Chain Reaction, and Analysis of In Vitro Precursor Cell Migration

Forebrains of E15.5 WT and Nogo-A KO embryos were dissociated for isolation of neural precursor cells following a previously described procedure (Leone et al. 2005). Briefly, neurospheres were cultured in DMEM/F12 supplemented with 50 μg/mL gentamycin (Gibco, Invitrogen, Carlsbad, CA), B27 (Invitrogen), 10 ng/mL epidermal growth factor (PeproTech EC Ltd., London, UK), and 20 ng/mL basic fibroblast growth factor (PeproTech). Fresh medium was added to the culture every 3 days, and long-term cultures were passaged every 5–7 days. To immuncytochemically characterize neurosphere-derived cells, 7- to 9-day-old neurospheres (passages 7–10) were plated on poly-D-lysine (PDL)–coated (5 μg/mL) coverslips in DMEM/F12 medium supplemented with gentamycin and B27. Forty-eight hours after plating, cells were used for immunostainings. For intracellular stainings, cells were washed after fixation in 4% PFA and then stained. For cell surface staining, cells were washed with phosphate-buffered saline (PBS), 1 mM $CaCl_2$, and 0.5 mM $MgCl_2$. Living cells were then incubated with the primary antibodies and fixed in 4% PFA, followed by primary antibody detection. Cell nuclei were counterstained with a green fluorescent Nissl stain (Molecular Probes, Invitrogen).

For reverse transcriptase polymerase chain reaction (RT-PCR), messenger RNA was isolated from WT or Nogo-A-deficient neurospheres (passage 7) and from neonatal WT brain (control). After being treated with rDNAse I (Ambion, Applied Biosystems, Rotkreuz, Switzerland), a reverse transcription and PCR were performed using Taqman Universal PCR Master Mix (Applied Biosystems). Primers used were the following: Nogo-A, U: 5′-TGCTTTGAATTATTCCAAGTAGTCC-3′, D: 5′-AGTGAGT-ACCCAGCTGCAC-3′; NgR, U: 5′-CTCGACCCCGAAGATGAAG-3′, D: 5′-TGTAGCACA CACAAGCACCAG-3′; p75, U: 5′-TAGAAGCTGAGCGCT-GTCGC-3′, D: 5′-CACACACGGTCTGGTTGGCT-3′; Lingo-1, U: 5′-TGCC-CCCACCTGGTTACAGA-3′, D: 5′-CATGCCAGATCCCAGAGGGA-3′; and TROY, U: 5′-ACAGGACGGTGCTCTTCGCT-3′, D: 5′-CAGGTCCGCGCA-CTGTTTGCAG-3′.

PCR was performed at an annealing temperature of 56 °C for 35 cycles. Analysis of PCR products was done after electrophoresis on a 1% agarose gel.

To study the migration of neurosphere-derived cells, time-lapse imaging was performed 15 h after plating of 7- to 9-day-old neurospheres (passages 7–10). We compared WT precursor cells, Nogo-A-deficient precursor cells, and cells from WT and Nogo-A KO embryos treated with anti-Nogo-A antibody 11C7 (Oertle et al. 2003; Liebscher et al. 2005), anti-Lingo-1 antibody (Novartis, Basle, Switzerland), anti-NgR antibody (R&D systems, Minneapolis, MN), or a mouse anti-immunoglobulin G (IgG) antibody (Novartis) as control (30 μg/mL). Antibodies were added to the medium 2 h before recording. Live cell imaging was performed using a Leica WideField IRBE microscope equipped with a climate chamber, a software automation (Improvision Openlab, PerkinElmer, Waltham, MA), and a high-sensitivity digital camera (Hamamatsu ORKA ER, HAMAMATSU PHOTONICS France SARL, Massy, France). Images were captured every 500 s. In total, 50 snapshots of different neurospheres were taken. For each experimental group, approximately 70–100 cells (from 3 independent experiments) were tracked during 7 h of video recording. Movies were further processed with the OpenLab and QuickTime software (Apple, Cork, Republic of Ireland). The distance covered by the imaged cells was calculated using ImageJ software (National Institutes of Health, Bethesda, MD).

Cell Adhesion and Spreading Assay

To test whether the highly inhibitory Nogo-A region, Nogo-delta20 (Oertle et al. 2003), affects neural precursor cell spreading, glass coverslips (1 cm²) were coated with poly-D-lysine (5 μg/mL), washed 3 times, and subsequently coated with different concentrations of Nogo-delta20 (50 and 100 pmol, diluted in PBS) for 1 h at 37 °C. Unbound Nogo-delta20 was removed by 3 washes with PBS. To evaluate whether spreading of neurosphere-derived cells is affected by fresh brain extract obtained from E18.5 WT and Nogo-A KO mouse embryos, glass coverslips were coated with different concentrations of forebrain CHAPS-extracted material. Unbound coating material was removed by 3 washes with PBS. Forebrains of E15.5 WT and Nogo-A KO embryos were dissociated for isolation of neural precursor cells as described above. Cells were plated at a density of 8000 cells/cm² in DMEM/F12/ N2 supplemented with B27, cultured for 1 h, fixed with 4% PFA, and then scored. The average number of adhered and spread cells on the control substrates (PDL or glass), Nogo-delta20, or brain extract, respectively, was determined using a phase contrast Olympus IMT2 microscope and F-View camera (Soft Imaging Systems, Olympus Soft Imaging Solutions GmbH, Münster, Germany) at 20× by counting in 5 randomly chosen fields of view of the coverslips.

In Vivo BrdU Labeling and Analysis of Cortical Neuron Migration

Pregnant WT and Nogo-A KO mice were intraperitoneally injected with BrdU (Sigma-Aldrich 50 mg/kg in sterile saline) every hour for a period of 3 h at stage E15.5.

For analysis of neuronal migration, ImageJ software (National Institutes of Health) was used. To quantify the density and distribution of BrdU⁺ cells by densitometric measurement, 2 adjacent bins were assessed covering the ventricular zone (VZ), the subventricular zone (SVZ), the intermediate zone (IZ), the subplate (SP), the cortical plate (CP), and the marginal zone (MZ). The bins corresponded to VZ/SVZ/ IZ and SP/CP/MZ for E17.5 and VZ/SVZ/IZ/SP and CP/MZ for E19. Region borders were defined using Tbr1 immunostaining since SP neurons are positive for this neuronal marker (Hevner et al. 2001). For E17.5, the distribution of the BrdU⁺ cells along the cortex width was analyzed by an additional densitometric measurement using the Leica AF6000 microscope (10× objective) and software. Five lines per coronal brain section were placed starting from the ventricle and ending at the cortical surface. The average numbers of cells at respective distances from the ventricular surface were measured, and the values for VZ and SVZ are shown as curves. To quantify the density and distribution of migrated neurons, immunostaining using the layer-specific neuronal markers Tbr1 and Satb2 (Britanova et al. 2008) was evaluated. For quantification of the Tbr1⁺ cells, a bin covering a region in the lower CP was assessed by densitometric analysis in E19 WT and Nogo-A KO cortex using a Leica AF6000 microscope (10× objective) and software. For normalization of the densitometric measurements, the unspecific background staining of the brain sections was measured

at cortical areas where no BrdU⁺ or Tbr1⁺ cells—depending on the kind of immunostaining—were detectable. After normalization, the mean of the densitometric values of each area was set to 1 for WT mice. All other values were calculated as ratio of the WT mice value.

Satb2⁺ cells were counted in a bin placed over a region in the upper CP of the cortex using the Leica AF6000 microscope (40× objective) and ImageJ software.

To assess possible influences of a changed tangential migration pattern, we quantified the number of Calbindin⁺ cells in the SVZ or CP for WT and Nogo-A KO cortices at E17.5 and E19.

For BrdU analysis, cortices of 5 WT and 5 Nogo-A KO embryos at E17.5 and 12 WT and 11 Nogo-A KO embryos at E19 were used; for analysis of the expression of the neuronal markers Tbr1 and SatB2, 6 WT and 6 Nogo-A KO embryos were used; and for the Calbindin quantification, cortices of 5 WT and 5 Nogo-A KO embryos were used; 3 sections per animal were analyzed.

Statistical Analysis

Data are expressed as mean ± SEM. Statistical comparisons were performed using the appropriate test, unpaired Student's *t*-test, or analysis of variance, followed by the Tukey's test (GraphPad Prism, GraphPad Software Inc., CA). Significance was considered for $P < 0.05$.

Results

Nogo-A Is Expressed in Radial Glial Cells, Migrating Postmitotic as well as Postmigratory Neurons of the Embryonic Mouse Cortex

The Nogo-A expression pattern was assessed during forebrain development in mouse embryos. Nogo-A⁺ cells were detected in all cortical layers at E15.5 and E17.5 (Fig. 1A–C). Absence of staining in Nogo-A KO mice confirmed the specificity of the anti-Nogo-A antibody staining (Fig. 1D). To characterize Nogo-A⁺ cells, colabeling with specific lineage markers was performed (Fig. 1A–C).

Within the VZ, we observed Nogo-A labeling of low intensity in radially oriented processes. These Nogo-A⁺ processes were costained for nestin (Fig. 1C), showing that they are derived
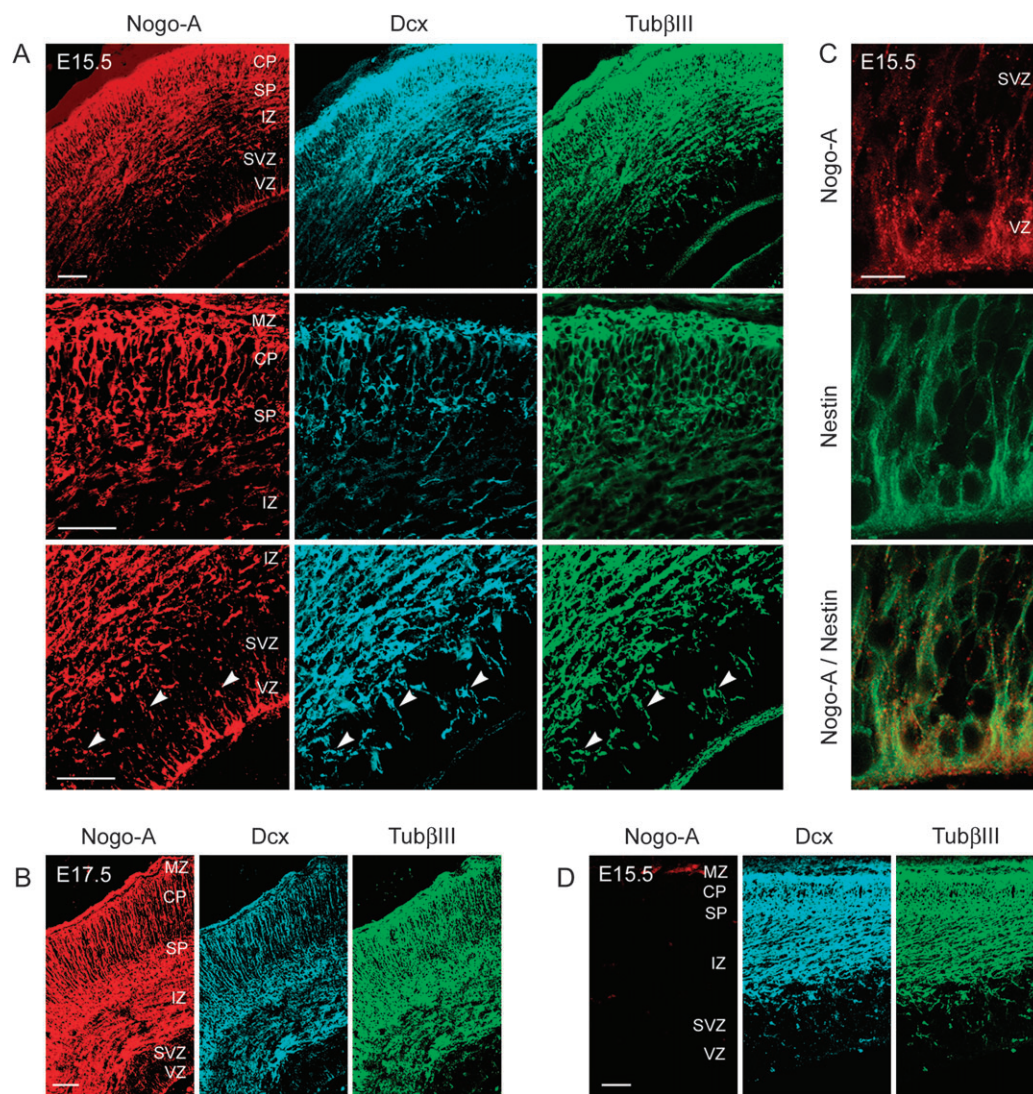

Figure 1. Nogo-A is expressed in radial glial cells, migrating postmitotic as well as postmigratory neurons of the embryonic mouse cortex. Colocalization of Nogo-A (red), Dcx (blue), and TubβIII (green) in radially (arrowheads) and tangentially migrating postmitotic and in postmigratory neurons of the E15.5 (A) and E17.5 (B) mouse cortex. (C) Colocalization of Nogo-A (red) and nestin (green) in radial glial cells within the VZ and SVZ of the E15.5 mouse cortex. (D) Absence of anti-Nogo-A immunostaining in the E15.5 Nogo-A KO mouse cortex showing the specificity of the immunostaining procedure. Scale bars: A, B, and D = 100 µm; C = 50 µm.

from radial glial cells. To study whether Nogo-A is important for the morphology of radial glial cells, we compared the pattern of nestin[+] radial processes in the developing cortex of WT and Nogo-A KO embryos. No major morphological differences of nestin[+] structures were observed between the 2 genotypes, suggesting that Nogo-A is not essential for the formation of the radial glial network in the developing cortex (Supplementary Fig. S1).

At E15.5 and E17.5, we found Nogo-A, Dcx, and TubβIII triple-positive cells in the SVZ, IZ, SP, CP, and MZ (Fig. 1A,B). Dcx and TubβIII double-labeled radially and tangentially migrating postmitotic cells in the SVZ and IZ showed different intensities of Nogo-A staining. Many of the early neurons with a radial orientation expressed Nogo-A in the cell body and to a lower degree in the processes (Supplementary Fig. S2A). Tangentially migrating neurons were strongly Nogo-A[+] in both the cell body and the processes (Supplementary Fig. S2B), an observation that confirms the finding by Mingorance-Le Meur et al. (2007). Prominent Nogo-A labeling was also detected in the majority of postmigratory neurons in the CP (Fig. 1A,B).

Nogo-A and the Nogo Receptor Components NgR, Lingo-1, TROY, and p75 Are Expressed in Embryonic Mouse Forebrain–Derived Neurospheres

Different studies suggest that neural stem cells isolated from embryonic forebrain–forming neurospheres in vitro correspond to precursor cells within the VZ (Jacques et al. 1998). We tested whether neurospheres express Nogo-A since they are derived from Nogo-A[+] radial glial cells.

Nogo-A transcript was detected by RT-PCR in neurospheres derived from E15.5 mouse brain (Fig. 2A). Since the known inhibitory effects of Nogo-A on neurite growth involve a multiprotein receptor complex containing the membrane proteins NgR, Lingo-1, p75 (Fournier and Strittmatter 2001; Wang et al. 2002; Mi et al. 2004), and/or the p75-related molecule TROY (Mandemakers and Barres 2005; Park et al. 2005; Shao et al. 2005), we analyzed whether these molecules are present in cells forming neurospheres. As for Nogo-A, we also found transcripts for NgR, Lingo-1, TROY, and p75 (Fig. 2A).

When neurospheres were plated on coverslips in a medium without growth factors, cells started to migrate away from the spheres within half a day. By immunostaining, we found that all migrating cells strongly expressed Nogo-A (Fig. 2B). The majority of migrating cells were positive for nestin, an intermediate filament usually expressed by precursor and radial glial cells (Fig. 2E), and only about 1% were positive for TubβIII (Fig. 2E). Immunostaining also revealed that nestin^{+} cells express Pax6, a radial glia marker (Fig. 2F). All migrating nestin[+] or TubβIII^{+} cells were positive for the Nogo receptor components NgR, Lingo-1, and p75 (Fig. 2D and Supplementary Fig. S3). In contrast, TROY was only present in nestin^{+} cells and not in TubβIII^{+} immature neurons.

When live cultures were stained with the anti-Nogo-A antibody, we found that Nogo-A was distributed in a punctate manner on the surface of the cells, similar to previous observations on dorsal root ganglion neurons (Dodd et al 2005) and oligodendrocytes (Oertle et al. 2003) (Fig. 2C). The specificity of the anti-Nogo-A antibody was confirmed by the absence of staining of cells isolated from Nogo-A KO mice (Fig. 2C). As an additional control for the specificity of the surface staining procedure using live cells, we applied 2 antibodies against the abundant intracellular proteins nestin or TubβIII.

The complete absence of staining with these 2 antibodies clearly demonstrated that only molecules localized on the cell surface were labeled with this procedure (data not shown).

Surface Nogo-A and Nogo-A Receptor Components Negatively Regulate the Motility of Migrating Neurosphere-Derived Cells

Twelve hours after plating the neurospheres on poly-D-lysine–coated coverslips, we recorded the migratory behavior of nestin[+], Nogo-A[+], and Nogo receptor^{+} cells using time-lapse imaging. Most cells migrated away from the neurospheres, but their movement was not continuous or linear over time. Pauses or migration in the reverse direction were frequently observed (Fig. 3B). Videos in the supplementary data (Supplementary Movies) show examples of such different behaviors. Because Nogo-A is present intracellularly as well as on the surface of neurosphere-derived cells (Fig. 2), we did not only compare the migration of cells derived from Nogo-A KO mice and WT cells but also used anti-Nogo-A function–blocking antibodies to assess whether the changes observed in the motility of Nogo-A–deficient cells were mediated by surface Nogo-A. The average distance covered by Nogo-A–deficient cells was significantly increased (76.47 μm ± 3.22/7 h, $n = 70$) compared with that of WT cells (64.45 μm ± 3.21/7 h, $n = 81$; Fig. 3C). When cells were treated with anti-Nogo-A antibody, the average distance covered by the migrating cells was also greater (95.22 μm ± 4.77/7 h, $n = 74$) compared with control antibody–treated WT cultures (64.66 μm ± 4.83/7 h, $n = 104$; Fig. 3F). Thus, the average distance covered was increased by 30% when surface Nogo-A was blocked by antibodies and at the same time higher than the distance covered by Nogo-A–deficient cells (Fig. 3C,F). This difference can be due to 2 reasons: Nogo-A–deficient cells migrate faster than WT cells or Nogo-A–deficient cells pause less or for a shorter time. We therefore measured the maximum speed of WT and Nogo-A–deficient cells and determined how frequently these cells were immobile for at least 500 s. No difference in the maximum speed was observed between WT cells (0.641 μm ± 0.041/min, $n = 81$) and Nogo-A–deficient cells (0.654 μm ± 0.036/min, $n = 70$; Fig. 3D), but the maximum speed of anti-Nogo-A antibody–treated cells was on average significantly higher (0.779 μm ± 0.036/min, $n = 74$) than that of cells with control antibody treatment (0.594 μm ± 0.033/min, $n = 104$). In addition, we found that Nogo-A–deficient cells paused less frequently (0.914 pauses ± 0.128/7 h, $n = 70$) than WT cells (1.346 pauses ± 0.161/7 h, $n = 81$; Fig. 3E) and also that anti-Nogo-A antibody–treated cells made fewer pauses than control antibody–treated cells (control: 1.269 pauses ± 0.115/7 h, $n = 104$; anti-Nogo-A: 0.892 pauses ± 0.106/7 h, $n = 74$; Fig. 3H). These data suggest that cessations of migratory movements are more frequent in the presence of Nogo-A. Taken together, the effect on the mobility of neurosphere-derived cells is likely mediated by cell surface Nogo-A.

At the time of the video analysis, that is, 12 h after plating of the neurospheres on PDL–coated dishes, the large majority of the migrating cells were nestin[+]. We then analyzed the differentiation of WT and Nogo-A KO cells after 7 days in differentiation medium by immunocytochemical stainings for neurons, astrocytes, and oligodendrocytes. The same proportions of all 3 CNS cell types were found in both WT and Nogo-A KO cultures: The cultures generated approximately 65% astrocytes (GFAP[+]), 20% neurons (TubβIII[+]), and 15% oligodendrocytes (APC[+]; Supplementary
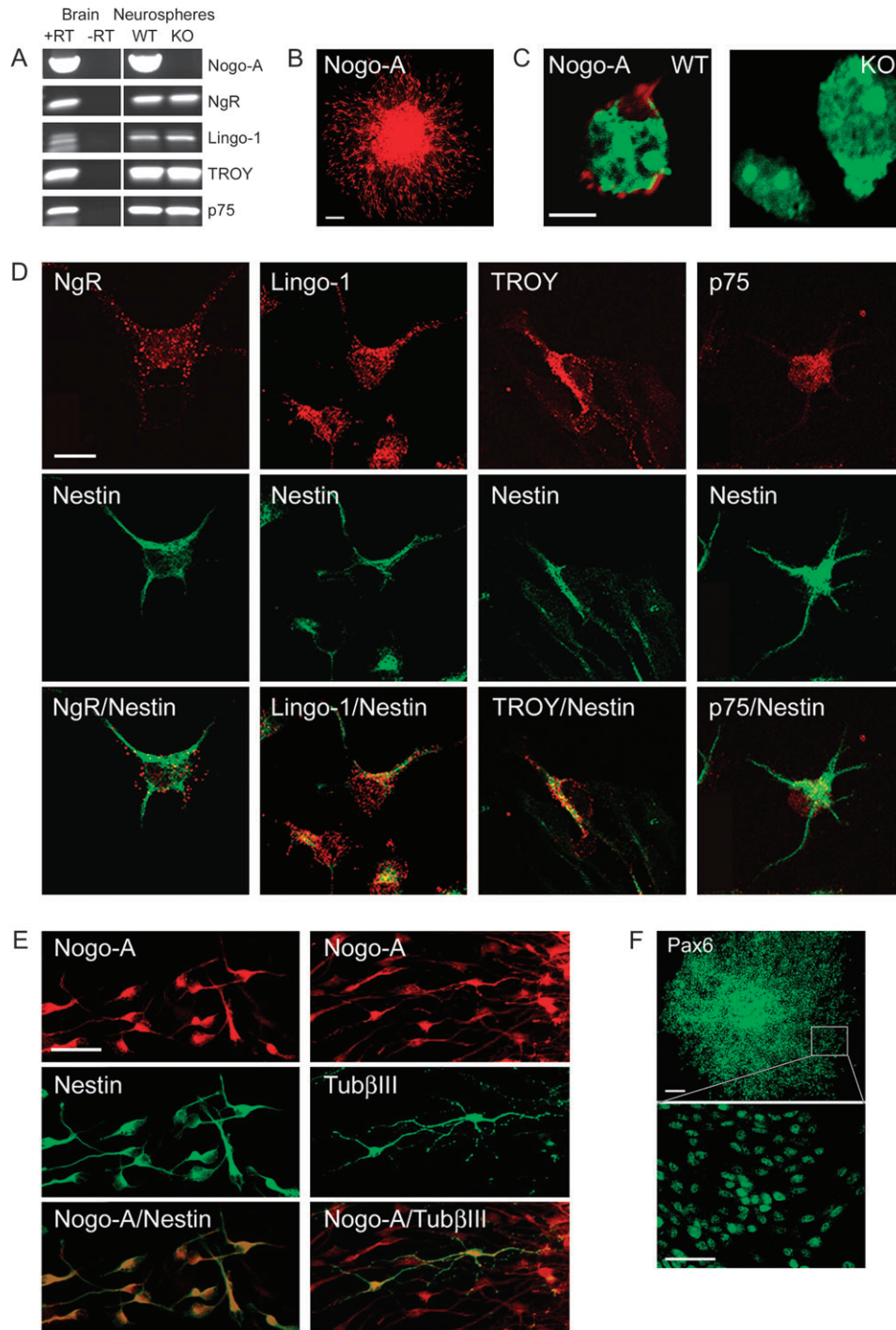
Figure 2. Nogo-A and the Nogo receptor components NgR, Lingo-1, TROY, and p75 are expressed by embryonic mouse forebrain–derived neurospheres. (A) Transcripts for Nogo-A, NgR, Lingo-1, TROY, and p75 are all detected by RT-PCR in E15.5 mouse forebrain–derived neurospheres (passage 5). Nogo-A is absent in Nogo-A KO mouse forebrain–derived neurospheres, but the receptor components persist. Total messenger RNA from neonatal mouse brain was used as a positive control. "+RT" and "−RT" indicate performance of reverse transcription with and without reverse transcriptase, respectively. (B) Nogo-A (red) immunoreactivity is found in precursor cells of a plated neurosphere cultured for 1 day without growth factors. Note the halo of migrating Nogo-A$^+$ cells surrounding the sphere. (C) Localization of Nogo-A (red) on the cell surface of WT mouse neurosphere-derived cells. No immunostaining was observed on cells derived from Nogo-A KO mouse embryos. Nuclei are counterstained with green fluorescent Nissl stain. (D) Colocalization of NgR, Lingo-1, TROY, or p75 (red) and nestin (green) in migrating precursor cells emanating from plated neurospheres. (E) Colocalization of Nogo-A (red) and nestin (green) or TubβIII (green) in migrating precursor cells emanating from plated neurospheres. Approximately 1% of migrating cells are positive for TubβIII. (F) Expression of the radial cell glial marker Pax6 (green) in almost all neurosphere-derived cells. Scale bars: B = 100 μm; C = 10 μm; D = 10 μm; E = 50 μm; F = 100 μm, 50 μm.

Fig. S4). The same proportions of astrocytes, neurons, and oligodendrocytes were also found in cultures of WT cells grown in the presence of the anti-Nogo-A antibody 11C7 or of a control antibody. Since no significant difference in fate specification was found when Nogo-A was knocked out or neutralized, we assume that the effects of Nogo-A on cell locomotion are not due to a change in the proportion of differentiated cells with different mobility during the period of live imaging.
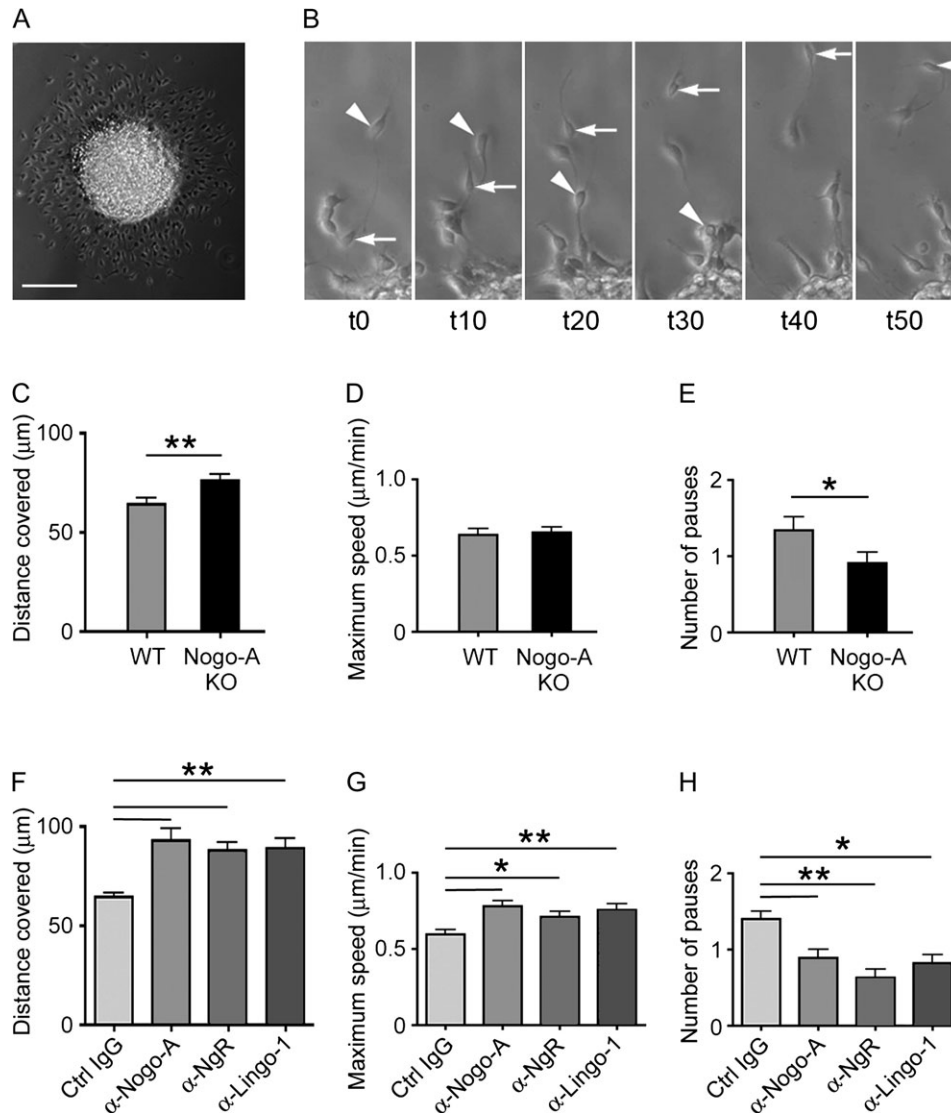
Figure 3. Surface Nogo-A and some Nogo-A receptor components negatively regulate the motility of migrating neurosphere-derived cells. (*A*) Phase contrast picture of a plated neurosphere cultured without growth factors for 1 day. Note the halo of migrating cells surrounding the sphere. (*B*) Example of a cell migrating away from the neurosphere (arrow) and of an emanated cell moving back toward the sphere (arrowhead). Time period from t_0 to t_{10} = 5000 s. (*C–E*) Quantification of the average distance (*C*) covered by migrating WT or Nogo-A KO mouse neurosphere cells, the maximum speed (*D*), and the number of pauses (no movement for at least 500 s) (*E*). Bars represent mean ± SEM of 4 independent experiments (number of cells analyzed: WT: $n = 71$; Nogo-A KO: $n = 72$); **$P < 0.01$ and *$P < 0.05$, unpaired Student's t-test. (*F–H*) Quantification of the average distance (*F*) covered by migrating WT neurosphere cells treated with function-blocking anti-Nogo-A, anti-Lingo-1, anti-NgR, or control IgG (ctrl IgG) antibodies; the maximum speed (*G*); and the number of pauses (*H*). Bars represent mean ± SEM of 3 independent experiments (number of cells analyzed: anti-Nogo-A: $n = 55$; anti-Lingo-1: $n = 57$; anti-NgR: $n = 60$; and control IgG: $n = 154$); **$P < 0.01$ and *$P < 0.05$, analysis of variance, Tukey's test. Scale bar = 100 μm.

As described above, NgR and Lingo-1, 2 Nogo receptor components known to be involved in Nogo-mediated growth cone collapse and nerve fiber growth arrest (GrandPre et al. 2000; Oertle et al. 2003; Mi et al. 2004), were present in the nestin[+] neurosphere–derived cells (Fig. 2*D*). To test whether NgR and Lingo-1 play a role for the migration of precursor cells, we added function-blocking anti-NgR or anti-Lingo-1 antibodies to the neurosphere cultures. The total covered distance and the maximum speed of migration were increased, and the number of pauses was reduced with both antibodies, very similar to the results obtained with anti-Nogo-A antibodies (Fig. 3*F–H*). These data argue for a direct involvement of NgR and Lingo-1 in mediating the effects of Nogo-A on the migration of neurosphere-derived cells.

Exogenous Nogo-A Negatively Regulates Adhesion and Spreading of Embryonic Neural Precursor Cells

To study whether the effects of Nogo-A on cell motility are cell autonomous or substrate dependent, adhesion and spreading of neural precursor cells were evaluated on different substrates. Cell spreading was decreased by Nogo-delta20, the inhibitory region of Nogo-A, in contrast to the control substrate (Fig. 4*A*). We analyzed WT and Nogo-A KO precursor cells after they adhered on PDL-coated coverslips (control). Seventy-four percent of WT and 77% of Nogo-A KO precursor cells had spread after 1 h. Whereas a concentration of 50 pmol Nogo-delta20 did not decrease the number of spread cells significantly (74% of WT cells and 69% of Nogo-A KO cells), 100 pmol Nogo-delta20 inhibited the spreading of WT as well as Nogo-A KO
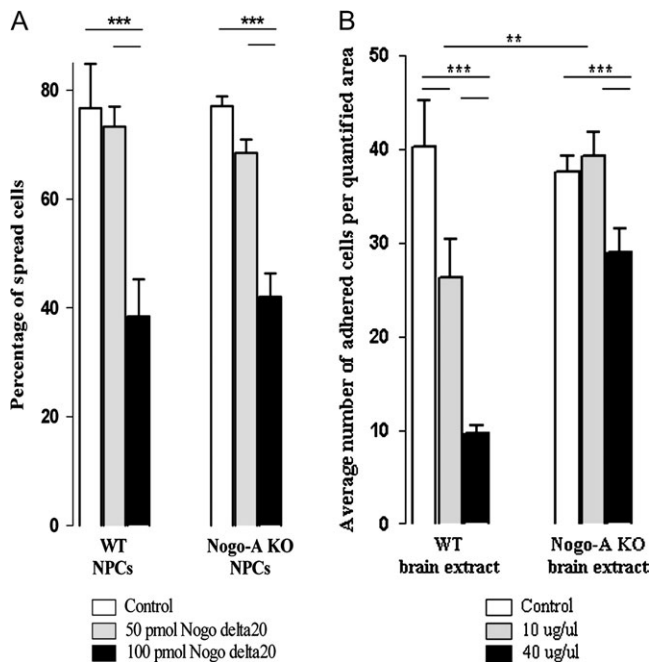
Figure 4. Nogo-A negatively regulates adhesion and spreading of embryonic neural precursor cells. Quantification of the proportions of WT and Nogo-A KO neural precursor cells plated on different concentrations of Nogo-delta20 or fresh brain extract from WT or Nogo-A KO mouse embryos. (*A*) Cells on control substrate (PDL) or on 50 pmol Nogo-delta20 showed normal spreading behavior after 1 h, while WT as well as Nogo-A KO precursor cells plated on a higher concentration of 100 pmol Nogo-delta20 showed a significant decrease in spreading. (*B*) A concentrations of 10 μg/μL brain extract caused a significant decrease in cell adhesion of WT and Nogo-A KO precursor cells compared with control substrate. Ten micrograms per microliter Nogo-A KO brain extract, however, did not inhibit spreading of WT precursor cells. At 40 μg/μL, WT brain extract had a very strong inhibitory effect on precursor cell adhesion for both genotypes, whereas Nogo-A KO mouse brain extract impaired adhesion only mildly, probably through other repulsive molecules present in the extract. Bars represent mean ± SEM; ***$P < 0.001$ and **$P < 0.01$, unpaired Student's *t*-test.

neural precursor cells significantly (33% of WT cells and 41% of Nogo-A KO cells), with the majority of cells remaining round.

Adhesion of WT neurosphere-derived cells plated on a CHAPS protein extract of embryonic forebrain showed a difference depending on the genotype of the substrate/ extract (Fig. 4*B*). Whereas an average number of 40 cells adhered on noncoated glass coverslips (control), the adherence on 10 μg/μL embryonic WT brain extract was decreased by approximately 35%. In contrast, the same protein concentration of brain extract derived from Nogo-A KO mouse embryos did not change the adhesion of neural precursor cells compared with the control situation. A higher protein concentration (40 μg/μL) of WT mouse brain extract decreased the adhesion of cells by approximately 75%. A much weaker (20%) anti-adhesive effect was seen on Nogo-A KO brain extract, probably due to other repulsive/anti-adhesive molecules present in the extract.

Nogo-A Regulates the Radial Migration of Cortical Neurons In Vivo

To assess a possible role of Nogo-A during radial migration of cortical neurons in vivo, we injected BrdU into pregnant mice at E15.5. We examined the distribution of a cohort of migrating neurons generated at E15.5 in the embryonic motor cortex at E17.5 and E19. The total number of BrdU^{+} cells and the BrdU

intensity were similar in WT and Nogo-A KO cortices, suggesting that proliferation and survival of cells are not affected by the absence of Nogo-A (Fig. 5*D,E,I*). The distribution of BrdU^{+} cells in the developing cortex, however, differed between WT and Nogo-A KO mice. In the WT E17.5 cortex, the majority of the BrdU^{+} cells resided in the VZ and SVZ and a typical accumulation of BrdU^{+} cells was seen in a band between the VZ and IZ. This accumulation of migrating neuronal precursors was not found in the Nogo-A KO cortex where the labeled cells were more evenly distributed over the SVZ, the IZ, and the SP (Fig. 5*B,C,E*). At E19, optical densitometry revealed that significantly fewer neuronal precursors had reached the CP in the Nogo-A KO mice, whereas more BrdU^{+} cells were found in the VZ, SVZ, and IZ compared with WT cortex (Fig. 5*F–J*). These results reflect a disturbance or delay in the radial migration.

To exclude that the observed differences in the number of BrdU^{+} cells were caused by a disturbed migration of late-born interneurons, which are moving tangentially from the ganglionic eminence into the SVZ or CP/MZ, we compared the numbers of Calbindin^{+} cells in these regions between WT and Nogo-A KO mice. We did not detect any differences confirming the observation of Mingorance-Le Meur et al. (2007) (data not shown).

Immunostainings for layer-specific neuronal markers (Tbr1 and Satb2) were performed to quantify the density and distribution of migrated cortical neurons. Tbr1 is a marker for early-generated neurons located mainly in the deep cortical layers. Densitometric analysis of Tbr1-immunostained brain sections at E19 revealed that the density of early-generated deep layer cortical neurons did not significantly differ between WT and Nogo-A KO mice (Supplementary Fig. S5). Satb2 is a transcription factor expressed in the majority of late-generated cortical neurons that reside in future cortical layers II through IV. We quantified the number of Satb2^{+} cells in a region in the upper CP at E19 (Fig. 5*H*). WT mouse cortices had a higher number of Satb2^{+} cells in the quantified region than Nogo-A KO mouse cortices, albeit this difference was not statistically significant ($P = 0.13$; Fig. 5*J*).

Discussion

Myelin-derived Nogo-A is one of the major inhibitory molecules for axon outgrowth in the adult CNS. While it has been intensively studied in this context, its function in neurons, where it is prominently expressed during development, still remains unclear. The present results suggest that Nogo-A plays a role for the radial migration of cortical precursor cells: In vitro, surface Nogo-A negatively modulated the locomotion of precursor cells via the Nogo receptor constituents NgR and Lingo-1, and in vivo, the radial migration of neuronal precursors in the E15–19 forebrain was disturbed in Nogo-A KO mice.

During cortical development, Nogo-A is present in and on the surface of migrating and postmigratory neurons and in and on radial glial cells (Mingorance-Le Meur et al. 2007), a major source of neurons and glia (Gotz et al. 2002; Noctor et al. 2002; Rakic 2003) and an important guide for migrating cortical neurons (Rakic 1972; O'Rourke et al. 1992). The absence of Nogo-A in KO mice did not have a detectable effect on the overall architecture of the radial glial network. Radially and tangentially migrating postmitotic neurons located in the SVZ and IZ were Nogo-A positive, and it was present in high amounts in postmigratory neurons in the CP and MZ.
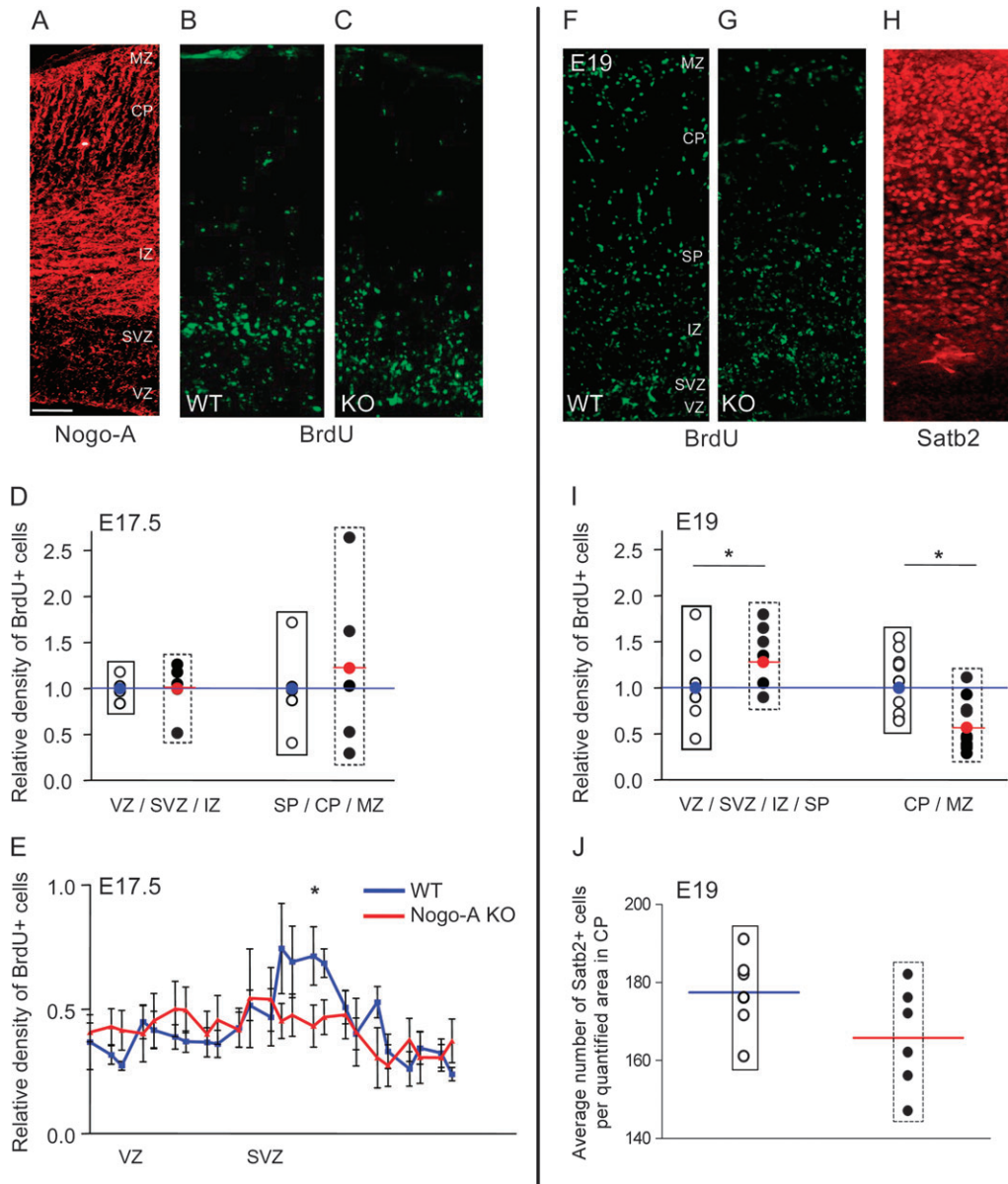
Figure 5. Nogo-A regulates the radial migration of cortical neurons in vivo. (*A–C*) E17.5 mouse cortices: Nogo-A expression pattern in a WT cortex (*A*), distribution of radially migrating neuronal precursor cells labeled with BrdU at E15.5 in WT (*B*), and Nogo-A KO (*C*). At E17.5, the accumulation of BrdU$^+$ cells in a band between the VZ and IZ, where postmitotic cells strongly express Nogo-A, was only detectable in the WT mouse cortex. In the Nogo-A KO mouse cortex, the newborn precursor cells were more dispersed in the SVZ and IZ. (*D* and *E*) Quantification of the distribution of BrdU$^+$ cells within the cortex at E17.5. (*D*) The number of BrdU$^+$ cells in both regions analyzed (VZ/SVZ/IZ and SP/CP/MZ) was not significantly different between the genotypes. (*E*) When we analyzed the distribution of BrdU$^+$ cells in the VZ and SVZ at higher resolution, we detected a significantly higher density of cells in the WT SVZ at E17.5. (*F* and *G*) E19 mouse cortices showing the distribution of radially migrating neuronal precursor cells labeled with BrdU at E15.5 in WT (*F*) and Nogo-A KO (*G*) embryos and Satb2 expression pattern in the WT cortex (*H*). (*I*) Densitometric measurements of BrdU$^+$ cells at E19 revealed that in the Nogo-A KO mouse, significantly less cells reached the upper cortical layers (CP/MZ); at the same time, more BrdU$^+$ cells remained in the lower layers (VZ/SVZ/IZ/SP) reflecting a delay in radial migration. (*J*) Cell counts in the upper CP show that the number of Satb2$^+$ cells tends to be lower in Nogo-A KO compared with WT mouse embryos at E19. Black circles represent individual Nogo-A KO animals as relative values compared with the average of the WT animals (open circles; average set to 1, blue line). The red circle and line represent the average density for the Nogo-A KO mice (black circles) at the given distance. Bars and curves represent mean ± SEM; *$P < 0.05$, unpaired Student's *t*-test. Scale bar = 100 μm.

We studied the possible role of Nogo-A for the migration of nestin$^+$ neural precursor cells. RT-PCR and immunofluorescence showed the presence of Nogo-A and the Nogo receptor components NgR, Lingo-1, TROY, and p75 in neurosphere-derived precursor cells. Live imaging revealed that Nogo-A–deficient cells migrated over a longer distance within a given time window compared with WT cells, mainly because they paused less. A similar but more explicit result was obtained by acute neutralization of Nogo-A by function-blocking antibodies. Importantly, anti-Nogo-A antibody–treated cells also showed a higher migration speed compared with control cells. Identical results were obtained with antibodies against the Nogo receptor components NgR or Lingo-1. Together, the data suggest that Nogo-A acts as a negative regulator or "brake" for migrating cortical precursors. This effect is mediated by surface Nogo-A via a receptor complex that includes the components NgR and

Lingo-1. The antibody effects may be direct by steric hindrance of the Nogo-A-binding site or indirect by internalization and downregulation of Nogo-A or its receptor complex as it has been shown in vitro and in vivo (Weinmann et al. 2006). The more pronounced effects of the antibodies compared with the genetic ablation of Nogo-A may be due to the absence of compensatory reactions, for example, upregulation of other inhibitory factors, known to occur in many KO models.

The overall migration-enhancing effect by Nogo-A absence or blockade observed here could be due to a decrease in contact inhibition of locomotion (Abercrombie 1979). Recently, Nogo-A was shown to inhibit the migration of olfactory ensheathing cells through NgR and subsequent activation of RhoA (Su et al. 2007). RhoA is a crucial mediator of Nogo-A–induced growth cone collapse and neurite growth inhibition (Fournier et al. 2003; Schwab 2004). LimK-1, slingshot, and cofilin downstream of RhoA are important effectors leading to cytoskeletal reorganization and in particular to disassembly of the actin cytoskeleton (Hsieh et al. 2006, Montani et al. 2009). RhoA is known to be highly expressed during corticogenesis (Olenik et al. 1999) and to be involved in the regulation of cell adhesion and migration (Fukata et al. 2003). A significant increase in RhoA activity was also detected during collision of migrating neural crest cells (which express Nogo-A; unpublished observations); inhibition of Rock, a downstream target of RhoA, led to a loss of contact inhibition of locomotion of these cells, implicating RhoA as a downstream effector of contact inhibition in these peripheral neural precursors (Carmona-Fontaine et al. 2008).

To assess whether the effect of Nogo-A on cell migration was cell autonomous or substrate dependent, we plated WT and Nogo-A^{+} precursor cells on Nogo-delta20 or on brain extract derived from WT or Nogo-A–deficient embryonic forebrain. Adhesion as well as spreading were markedly reduced by Nogo-delta20 in all precursor cells, with WT cells reacting equally to Nogo-A KO precursors. WT brain extract inhibited the adhesions of precursor cells already at low concentrations, whereas Nogo-A KO brain extract exerted an anti-adhesive effect only at a high concentration and to a much lower extent than the WT substrate. We conclude from these results that the effects of Nogo-A on precursor cell migration are mainly exerted by the Nogo-containing substrate and less dependent on intracellular Nogo-A in the precursor cells themselves.

Our in vivo studies showed a disturbed migration pattern of radially migrating cortical neurons born at E15.5. This disturbance was seen at E17.5 and E19 but was no longer obvious in the adult. A recent report showed that in Nogo-A/B/C-deficient mice, the tangential migration of early-born interneurons derived from the ventrally located eminentia mediana into the cortex was delayed (Mingorance-Le Meur et al. 2007). The KO mice used, Nogo-A specific versus Nogo-A/B/C KO, and the developmental time points analyzed are different in the 2 reports. However, both studies show a role of Nogo for the migration of neuronal precursor cells in the developing mouse cortex. Corroborating the findings for late-born tangentially migrating interneurons (Mingorance-Le Meur et al. 2007), we did not detect any differences in the number of Calbindin^{+} cells between the WT and Nogo-A KO cortical areas we analyzed, indicating that the different distribution of BrdU^{+} cells within the cortex at E15.5–E19 was exclusively due to radially migrating neurons.

The disturbances of the in vivo radial migration pattern of neuronal precursor cells in the Nogo-A KO E15–19 mouse cortex are complex and difficult to understand in detail at present. We excluded an effect of Nogo-A on neural precursor cell proliferation by quantifying the total number of BrdU^{+} cells, which was not significantly different between WT and KO in the embryonic mouse cortex at E17.5. Cortical migration is a multistage process with 4 distinct phases of migration in which neurons change shape and direction of movement (Kriegstein 2005). After being born in the VZ, neurons move radially away from the ventricle to the SVZ and remain there for as long as 24 h. In fact, we detected an accumulation of BrdU^{+} cells at E17.5 in the form of a band between the VZ and IZ in the WT mouse cortex. The band corresponds to a zone that is enriched for Nogo-A expressed mainly by early neurons in the SVZ/IZ. In the Nogo-A KO mouse cortex, the newborn precursor cells were more dispersed over these layers, not forming such a distinct band. This could be due to the absence of a repulsive "boundary effect" normally exerted by Nogo-A in the WT SVZ. Subsequent to their pause in the SVZ, the newborn precursors often move back toward the ventricle (Kriegstein 2005). Finally, the cells associate with radial glial fibers to migrate to the outer layers of the CP, their final destination. At E19, cells labeled by BrdU at E15.5 in the Nogo-A KO mouse cortex had migrated less far into the CP than WT cells. Although we observed a higher motility of Nogo-A–deficient precursors in vitro, important directional cues required for radial in vivo migration may be disturbed in the Nogo-A KO mice. Thus, Nogo-A repulsive forces might initially help to restrict neurons to the SVZ and guide them back into the VZ, and Nogo-A expression in radial glial cells and neurons could play a role in the balance between adhesion and repulsion during directed movement of the cells along the radial glial fibers. Nogo-A deficiency could lead to over adhesive interactions, thereby slowing the radial migration.

Interestingly, in the postnatal cortex of the Nogo-A KO mice, we did not detect any major abnormalities, although a surprisingly high interindividual variability in the cell density of layers II–IV neurons was observed, perhaps pointing to incomplete compensatory mechanisms (data not shown).

In conclusion, we found that Nogo-A, well studied for its inhibitory function on axon growth in the adult CNS, plays a role in the regulation of the radial migration of cortical neuronal precursor cells in development. We did not find indications that processes such as precursor cell proliferation, differentiation, or survival are changed in absence of Nogo-A. Our data suggest that the effects of Nogo-A on migration are mediated by cell surface Nogo-A through a receptor complex that includes NgR and Lingo-1. Many mechanistic details remain to be studied, in particular, how and where these different players interact with each other in vivo during cortical development. The migration of newborn neurons is finely regulated by multiple adhesive/attractive molecules, for example, integrins, cell adhesion molecules, cadherins, and netrins as well as repulsive cues, for example, neuropilins/semaphorins, Slit/Robo, or ephrins (Marin and Rubenstein 2003; Chen et al. 2008). The present results show that Nogo-A can be included in the growing family of instructive cues regulating neuronal migration and axon growth during development and in the adult CNS.

Supplementary Material

Supplementary materials can be found at http://www.cercor .oxfordjournals.org/.

Notes

References

Abercrombie M. 1979. Contact inhibition and malignancy. Nature. 281:259-262.

Al Halabiah H, Delezoide AL, Cardona A, Moalic JM, Simonneau M. 2005. Expression pattern of NOGO and NgR genes during human development. Gene Expr Patterns. 5:561-568.

Britanova O, de Juan Romero C, Cheung A, Kwan KY, Schwark M, Gyorgy A, Vogel T, Akopov S, Mitkovski M, Agoston D, et al. 2008. Satb2 is a postmitotic determinant for upper-layer neuron specification in the neocortex. 57:378-392.

Caltharp SA, Pira CU, Mishima N, Youngdale EN, McNeill DS, Liwnicz BH, Oberg KC. 2007. NOGO-A induction and localization during chick brain development indicate a role disparate from neurite outgrowth inhibition. BMC Dev Biol. 7:32.

Carmona-Fontaine C, Matthews HK, Kuriyama S, Moreno M, Dunn GA, Parsons M, Stern CD, Mayor R. 2008. Contact inhibition of locomotion in vivo controls neural crest directional migration. Nature. 456:957-961.

Caroni P, Schwab ME. 1988. Two membrane protein fractions from rat central myelin with inhibitory properties for neurite growth and fibroblast spreading. J Cell Biol. 106:1281-1288.

Chen G, Sima J, Jin M, Wang KY, Xue XJ, Zheng W, Ding YQ, Yuan XB. 2008. Semaphorin-3A guides radial migration of cortical neurons during development. Nat Neurosci. 11:36-44.

Chen MS, Huber AB, van der Haar ME, Frank M, Schnell L, Spillmann AA, Christ F, Schwab ME. 2000. Nogo-A is a myelin-associated neurite outgrowth inhibitor and an antigen for monoclonal antibody IN-1. Nature. 403:434-439.

Dodd DA, Niederoest B, Bloechlinger S, Dupuis L, Loeffler JP, Schwab ME. 2005. Nogo-A, -B, and -C are found on the cell surface and interact together in many different cell types. J Biol Chem. 280:12494-12502.

Fournier AE, Strittmatter SM. 2001. Repulsive factors and axon regeneration in the CNS. Curr Opin Neurobiol. 11:89-94.

Fournier AE, Takizawa BT, Strittmatter SM. 2003. Rho kinase inhibition enhances axonal regeneration in the injured CNS. J Neurosci. 23:1416-1423.

Fukata M, Nakagawa M, Kaibuchi K. 2003. Roles of Rho-family GTPases in cell polarisation and directional migration. Curr Opin Cell Biol. 15:590-597.

Gonzenbach RR, Schwab ME. 2008. Disinhibition of neurite growth to repair the injured adult CNS: focusing on Nogo. Cell Mol Life Sci. 65:161-176.

Gotz M, Hartfuss E, Malatesta P. 2002. Radial glial cells as neuronal precursors: a new perspective on the correlation of morphology and lineage restriction in the developing cerebral cortex of mice. Brain Res Bull. 57:777-788.

GrandPre T, Nakamura F, Vartanian T, Strittmatter SM. 2000. Identification of the Nogo inhibitor of axon regeneration as a Reticulon protein. Nature. 403:439-444.

Hevner RF, Shi L, Justice N, Hsueh Y-P, Sheng M, Smiga S, Bulfone A, Goffinet AM, Campagnoni AT, Rubenstein JLR. 2001. Tbr1 regulates differentiation of the preplate and layer 6. Neuron. 29:353-366.

Hirano S, Suzuki ST, Redies C. 2003. The cadherin superfamily in neural development: diversity, function and interaction with other molecules. Front Biosci. 8:d306-d355.

Hsieh SH, Ferraro GB, Fournier AE. 2006. Myelin-associated inhibitors regulate cofilin phosphorylation and neuronal inhibition through LIM kinase and Slingshot phosphatase. J Neurosci. 26:1006-1015.

Huber AB, Weinmann O, Brosamle C, Oertle T, Schwab ME. 2002. Patterns of Nogo mRNA and protein expression in the developing and adult rat and after CNS lesions. J Neurosci. 22:3553-3567.

Hunt D, Coffin RS, Prinjha RK, Campbell G, Anderson PN. 2003. Nogo-A expression in the intact and injured nervous system. Mol Cell Neurosci. 24:1083-1102.

Jacques TS, Relvas JB, Nishimura S, Pytela R, Edwards GM, Streuli CH, ffrench-Constant C. 1998. Neural precursor cell chain migration and division are regulated through different beta1 integrins. Development. 125:3167-3177.

Josephson A, Widenfalk J, Widmer HW, Olson L, Spenger C. 2001. NOGO mRNA expression in adult and fetal human and rat nervous tissue and in weight drop injury. Exp Neurol. 169:319-328.

Kadowaki M, Nakamura S, Machon O, Krauss S, Radice GL, Takeichi M. 2007. N-cadherin mediates cortical organization in the mouse brain. Dev Biol. 304:22-33.

Klein R. 2004. Eph/ephrin signaling in morphogenesis, neural development and plasticity. Curr Opin Cell Biol. 16:580-589.

Kriegstein AR. 2005. Constructing circuits: neurogenesis and migration in the developing neocortex. Epilepsia. 46(Suppl 7):15-21.

Leone DP, Relvas JB, Campos LS, Hemmi S, Brakebusch C, Fassler R, Ffrench-Constant C, Suter U. 2005. Regulation of neural progenitor proliferation and survival by beta1 integrins. J Cell Sci. 118:2589-2599.

Liebscher T, Schnell L, Schnell D, Scholl J, Schneider R, Gullo M, Fouad K, Mir A, Rausch M, Kindler D, et al. 2005. Nogo-A antibody improves regeneration and locomotion of spinal cord-injured rats. Ann Neurol. 58:706-719.

Mandemakers WJ, Barres BA. 2005. Axon regeneration: it's getting crowded at the gates of TROY. Curr Biol. 15:R302-R305.

Marin O, Rubenstein JL. 2003. Cell migration in the forebrain. Annu Rev Neurosci. 26:441-483.

Martinez A, Soriano E. 2005. Functions of ephrin/Eph interactions in the development of the nervous system: emphasis on the hippocampal system. Brain Res Brain Res Rev. 49:211-226.

Mi S, Lee X, Shao Z, Thill G, Ji B, Relton J, Levesque M, Allaire N, Perrin S, Sands B, et al. 2004. LINGO-1 is a component of the Nogo-66 receptor/p75 signaling complex. Nat Neurosci. 7:221-228.

Mingorance-Le Meur A, Zheng B, Soriano E, del Rio JA. 2007. Involvement of the myelin-associated inhibitor Nogo-A in early cortical development and neuronal maturation. Cereb Cortex. 17:2375-2386.

Mingorance A, Fontana X, Sole M, Burgaya F, Urena JM, Teng FY, Tang BL, Hunt D, Anderson PN, Bethea JR, et al. 2004. Regulation of Nogo and Nogo receptor during the development of the entorhino-hippocampal pathway and after adult hippocampal lesions. Mol Cell Neurosci. 26:34-49.

Montani L, Gerrits B, Gehrig P, Kempf A, Dimou L, Wollscheid B, Schwab ME. 2009. Neuronal Nogo-A modulates growth cone motility via Rho-TP/LIMK1/cofilin in the unlesioned adult nervous system. J Biol Chem. 284:10793-10807.

Noctor SC, Flint AC, Weissman TA, Wong WS, Clinton BK, Kriegstein AR. 2002. Dividing precursor cells of the embryonic cortical ventricular zone have morphological and molecular characteristics of radial glia. J Neurosci. 22:3161-3173.

O'Neill P, Whalley K, Ferretti P. 2004. Nogo and Nogo-66 receptor in human and chick: implications for development and regeneration. Dev Dyn. 231:109-121.

O'Rourke NA, Dailey ME, Smith SJ, McConnell SK. 1992. Diverse migratory pathways in the developing cerebral cortex. Science. 258:299-302.

Oertle T, van der Haar ME, Bandtlow CE, Robeva A, Burfeind P, Buss A, Huber AB, Simonen M, Schnell L, Brosamle C, et al. 2003. Nogo-A inhibits neurite outgrowth and cell spreading with three discrete regions. J Neurosci. 23:5393–5406.

Olenik C, Aktories K, Meyer DK. 1999. Differential expression of the small GTP-binding proteins RhoA, RhoB, Cdc42u and Cdc42b in developing rat neocortex. Brain Res Mol Brain Res. 70:9–17.

Park JB, Yiu G, Kaneko S, Wang J, Chang J, He XL, Garcia KC, He Z. 2005. A TNF receptor family member, TROY, is a coreceptor with Nogo receptor in mediating the inhibitory activity of myelin inhibitors. Neuron. 45:345–351.

Prinjha R, Moore SE, Vinson M, Blake S, Morrow R, Christie G, Michalovich D, Simmons DL, Walsh FS. 2000. Inhibitor of neurite outgrowth in humans. Nature. 403:383–384.

Rakic P. 1972. Mode of cell migration to the superficial layers of fetal monkey neocortex. J Comp Neurol. 145:61-83.

Rakic P. 2003. Developmental and evolutionary adaptations of cortical radial glia. Cereb Cortex. 13:541–549.

Richard M, Giannetti N, Saucier D, Sacquet J, Jourdan F, Pellier-Monnin V. 2005. Neuronal expression of Nogo-A mRNA and protein during neurite outgrowth in the developing rat olfactory system. Eur J Neurosci. 22:2145–2158.

Schwab ME. 2004. Nogo and axon regeneration. Curr Opin Neurobiol. 14:118–124.

Schwab ME, Caroni P. 1988. Oligodendrocytes and CNS myelin are nonpermissive substrates for neurite growth and fibroblast spreading in vitro. J Neurosci. 8:2381–2393.

Shao Z, Browning JL, Lee X, Scott ML, Shulga-Morskaya S, Allaire N, Thill G, Levesque M, Sah D, McCoy JM, et al. 2005. TAJ/TROY, an orphan TNF receptor family member, binds Nogo-66 receptor 1 and regulates axonal regeneration. Neuron. 45:353–359.

Simonen M, Pedersen V, Weinmann O, Schnell L, Buss A, Ledermann B, Christ F, Sansig G, van der Putten H, Schwab ME. 2003. Systemic deletion of the myelin-associated outgrowth inhibitor Nogo-A improves regenerative and plastic responses after spinal cord injury. Neuron. 38:201–211.

Spillmann AA, Bandtlow CE, Lottspeich F, Keller F, Schwab ME. 1998. Identification and characterization of a bovine neurite growth inhibitor (bNI-220). J Biol Chem. 273:19283–19293.

Su Z, Cao L, Zhu Y, Liu X, Huang Z, Huang A, He C. 2007. Nogo enhances the adhesion of olfactory ensheathing cells and inhibits their migration. J Cell Sci. 120:1877–1887.

Tozaki H, Kawasaki T, Takagi Y, Hirata T. 2002. Expression of Nogo protein by growing axons in the developing nervous system. Brain Res Mol Brain Res. 104:111–119.

Wang X, Chun SJ, Treloar H, Vartanian T, Greer CA, Strittmatter SM. 2002. Localization of Nogo-A and Nogo-66 receptor proteins at sites of axon-myelin and synaptic contact. J Neurosci. 22:5505–5515.

Weinmann O, Schnell L, Ghosh A, Montani L, Wiessner C, Wannier T, Rouiller E, Mir A, Schwab ME. 2006. Intrathecally infused antibodies against Nogo-A penetrate the CNS and downregulate the endogenous neurite growth inhibitor Nogo-A. Mol Cell Neurosci. 32:161–173.

Yiu G, He Z. 2006. Glial inhibition of CNS axon regeneration. Nat Rev Neurosci. 7:617-627.